The Dexterity Analysis of a Spatial Three-Degree of Freedom Parallel Manipulator with Constrained Branch

Haiqiang Zhang, Hairong Fang, Bingshan Jiang, and Shuaiguo Wang

***Abstract*—This paper presents a spatial three-degree of freedom (DOF) 3-PUS-UP parallel manipulator with constrained branch that can be employed to high-speed milling for large heterogeneous complex structural component in aerospace field. Taking full consideration of the influence of the actuated branches, the serial constrained branch and the parasitic motion of the terminal moving platform, the closed-loop vector method is employed to deduce the kinematic position inverse solution, the actuation Jacobian matrix and the constrained Jacobian matrix are obtained by resorting to the screw theory and the D-H method, and the uniform full rank Jacobian matrix is constructed. With the help of the matrix condition number and matrix norm theory, the dexterity index characterizing the comprehensive transmission performance of the parallel manipulator is formulated. The distribution pattern of the performance index of the 3-PUS-UP parallel manipulator in the workspace is depicted by some cases, and the performance distribution of the mechanism is briefly investigated, and the optimum workspace region of the dexterity is then drawn in detail. The research results illustrate that the 3-PUS-UP parallel manipulator has good kinematic dexterity, which can be applied to the precision assembly, hybrid machine tool milling, and automobile spraying. Simultaneously, thus it also has a good prospect in engineering application.**

***Index Terms*—Parallel manipulator, Jacobian matrix, dexterity, condition number, optimum workspace.**

I. Introduction

The spatial lower mobility parallel manipulator, especially the 1T2R three-degree of freedom (T denotes the translation, and R denotes the rotation) parallel manipulator as the main spindle of the high-end intelligent equipment, has been widely applied to the equal thickness machining of the complex components in the aerospace and automobile field, and the assembly of the aeronautical aluminum structure [1]-[3]. The typical successful applications include Sprint Z3 head [4], Tricept hybrid machine tool [5], Exechon hybrid machine tool [6], and so on. In order to ensure that the parallel manipulator can complete the complex machining task and take full advantage of excellent kinematic and dynamic comprehensive performance, the parallel manipulator with constrained branch and the redundant actuated parallel manipulator are usually adopted [7]-[9]. The suitable constrained branch does not provide the actuation, which determines the DOF of the mechanism. While the redundant actuation that the number of actuator is larger than the degree of freedom required by actual tasks can't change the DOF of the parallel manipulator, yet which can effectively improve the accuracy and kinematic characteristics of the parallel manipulator. In the practical and potential applications, to increase the workspace of the 1T2R parallel manipulator, a large moving guide rail can be in serial. At the same time, it is of crucial importance significance to improve the orientation capability, the two or three degree of freedom turning head can be connected to the moving platform, and then the multi-degree of freedom hybrid manipulator with larger workspace can be utilized as the five-axis hybrid kinematic machine (HKM) [10].

In recent years, the 1T2R parallel manipulator has attracted increasing attentions in both academia and industry. The research focus is mainly on the configuration synthesis, kinematics and dynamics performance analysis and dimension evaluation [11], [12]. In the configuration synthesis, there exists a class of mechanism composed of suitable constrained branch and unconstrained active branches, such as Tricept [13]. According to the different constraint and actuation effect of the branched chain to the moving platform, the branched chain can be divided into unconstrained active branch, suitable constrained passive branch, and suitable constrained active branch [14]. In this paper, the middle branched chain with the suitable constrained branch is introduced, which only provides constraints to the moving platform and does not provide actuation. Li et al. [15] adopted the virtual chain method to classify the 1T2R parallel manipulator into four categories, that is, UP, PU, RPR and P^*U^* configuration, and made a summary to the current research progress at the same time. The kinematic position analysis of the 3-PUS-PU parallel manipulator is carried out by Gao, and the workspace, manipulability, dexterity and stiffness index are established, and multi-objective optimization design is performed [16]. The kinematic dexterity and stiffness performance of the three degrees of freedom 3-PUS-UP parallel manipulator with a constrained UP branched chain is analyzed in literature [17]. Merlet [18] pointed out that the Jacobian based indices (such as determinant, condition number and singular values) are not sound when they are applied to parallel manipulator with translational and rotational coupling degree of freedom, what's more, the inconsistency

Manuscript received May 6, 2018, revised June 11, 2018. This work was supported by the Central Universities under Grant No.2018JBZ007, No.2018YJS136, No.2017YJS158, China Scholarship Council (CSC) under Grant No.201807090079, and the National Natural Science Foundation of China (NSFC) under Grants 51675037.

Haiqiang Zhang and Bingshan Jiang are School of Mechanical, Electronic and Control Engineering, Beijing Jiaotong University, Beijing, P.R. China (e-mail: hqzhang@bjtu.edu.cn,17116381@bjtu.edu.cn).

Hairong Fang is with Beijing Jiaotong University and Robotics Research Center leader (e-mail: hrfang@bjtu.edu.cn).

Shuaiguo Wang is with the Mechanical Engineer, MH Robot & Automation Limited Company, Weifang, Shandong, P.R. China (e-mail: 13336362653@163.com).

DOI: 10.7763/IJET.2018.V10.1112

of unit of the elements in the Jacobain matrix leads to unclear physical meaning and coordinate dependence, which may cause erroneous interpretations. Therefore, the parallel manipulator with coupling degree of freedom can't employ its algebraic eigenvalues directly, it should be first processed by dimensional normalization. Huang et al. summarized two ways to measure the dexterity of the parallel manipulator [19], one is the condition number of the Jacobian matrix, and the other is the manipulability defined by Yoshikawa [20].

The present study focuses on a spatial three-degree of freedom 3-PUS-UP parallel manipulator utilized as hybrid kinematic machine, in accordance with the inverse kinematics analysis of the parallel manipulator, the paper aims to establish the unified Jacobian matrix, and further the condition and manipulability of the Jacobian matrix are applied as a measure of the dexterity for the proposed parallel manipulator. In consideration of specific application examples, the distribution atlases of the performance index of 3-PUS-UP parallel manipulator in the reachable workspace are depicted in detail. The research results illustrate that the proposed parallel manipulator has good kinematic dexterity and thus a suitable candidate for five-axis machining.

II. Kinematics Analysis

A. Architecture Description and Coordinate System Setting

The parallel manipulator proposed in this paper can also be designed as a hybrid kinematic machine, as shown in Fig. 1. This parallel manipulator is composed of a fixed platform, the moving platform and four branches connecting the fixed platform and the moving platform (Fig. 2). The fixed platform is connected to the moving platform through three identical actuation branches PUS and the intermediate constraint branch UP, where P, U, and S represent active prismatic joint, universal and spherical joint, respectively. The radius of the circumcircle of the moving platform is r_a, the fixed platform $B_1B_2B_3$ is the equilateral triangle, whose radius of circumcircle is r_a, the structure angle of the slide rail between the middle platform and the lower platform is α, and the slide block can move on the guide rail whose center point is C_1, C_2 and C_3. The slider and the fixed platform are connected by a universal joint, and the first axis is perpendicular to the guide rail, and the second axis is perpendicular to the first axis. The distance that the slider is s_i and its direction vector is $\mathbf{s}_{i0}$, the length of the constant rod is l_i and its direction vector is $\mathbf{l}_{i0}$, and the direction vector B_iA_i is $\mathbf{L}_i$.

For the purpose of facilitate analysis, as depicted in Fig. 2. A fixed coordinate system *B-xyz* attached to the fixed platform is set up, the origin *B* of the coordinate system *B-xyz* is a circle center with triangle $B_1B_2B_3$. The *x*-axis is parallel to the vector BB_1, the *z*-axis is perpendicular to the fixed platform upward, and *y*-axis direction is determined by the right rule. Similarly, a relative coordinate system *A-uvw* located to the moving platform is set up, the coordinate origin *A* is the geometric center of the moving platform. The *u*-axis is parallel to the vector AA_1, the *w*-axis is perpendicular to the moving platform upward, and the *v*-axis direction is determined by the right rule.

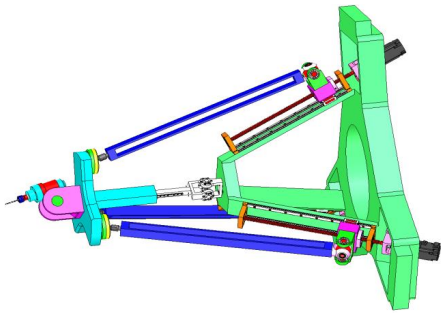

Fig.1. A 5-DOF hybrid kinematic machine

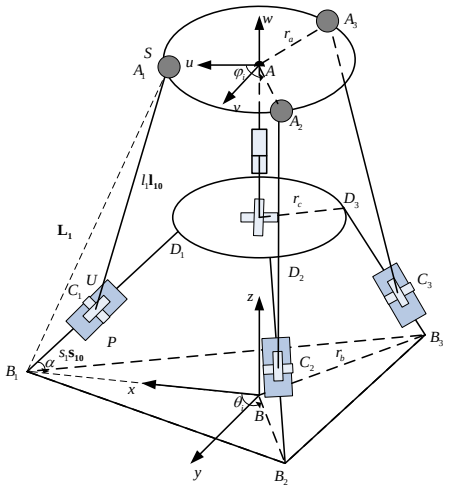

Fig. 2. Schematic diagram of the 3-PUS-UP parallel manipulator

B. Position Inverse Solution

The position inverse solution of the 3-PUS-UP parallel manipulator can be attributed to the known the structure parameters and positon vector of the point A, to solve the orientation of the moving platform and the required actuator inputs of the active prismatic joint [21].

The vector A_iB_i can be represented as in the fixed coordinate system $B-xyz$

$$\mathbf{L}_i = \mathbf{a}_i + \mathbf{r} - \mathbf{b}_i = l_i\mathbf{l}_{io} + s_i\mathbf{s}_{io} \tag{1}$$

where $\mathbf{b}_i = r_b[\mathrm{c}\varphi_i \quad \mathrm{s}\varphi_i \quad 0]^{\mathrm{T}}$, ${}^{p}\mathbf{a}_i = r_a[\mathrm{c}\varphi_i \quad \mathrm{s}\varphi_i \quad 0]^{\mathrm{T}}$, $\mathbf{a}_i = \mathbf{R}\,{}^{p}\mathbf{a}_i$, $\mathbf{s}_{io} = \left[-\mathrm{c}\theta_i\mathrm{c}\alpha \quad -\mathrm{s}\theta_i\mathrm{c}\alpha \quad \mathrm{s}\alpha\right]^{\mathrm{T}}$, $\mathbf{r} = [x, y, z]^{\mathrm{T}}$, and $\boldsymbol{r}$ denotes the position vector of point *A* in the coordinate system *B-xyz*, **R** represents the rotation matrix of the coordinate system A-*uvw* relative to the fixed coordinate system *B-xyz*, φ_i indicates the angle between the connection of joint A_i or B_i and the central joint of the coordinate system and the *x*-axis, and in which *s* and *c* are the abbreviation of *sine* and *cosine*, respectively.

Taking the norm on both sides of (1) leads directly to

$$s_i^2 - 2\mathbf{L}_i^{\mathrm{T}}s_{io}s_i + \mathbf{L}_i^{\mathrm{T}}\mathbf{L}_i - l^2 = 0 \tag{2}$$

Combining the position inverse solution about the linear displacement s_i of the active prismatic joint can be formed as

follows

$$s_i = \mathbf{L}_i^{\mathrm{T}} s_{io} \pm \sqrt{(\mathbf{L}_i^{\mathrm{T}} \mathrm{s}_{io})^2 - \mathbf{L}_i^{\mathrm{T}} \cdot \mathbf{L}_i + l^2} \tag{3}$$

C. Jacobian Matrix of the Parallel Component

According to the screw theory, the instantaneous velocity generated by the branch chain of i (i=1,2,3) can be expressed as [22]

$$\$_p = \begin{bmatrix} \omega & \upsilon \end{bmatrix}^{\mathrm{T}} = \dot{q}_i \$_{1,i} + \dot{\theta}_{2,i} \$_{2,i} + \dot{\theta}_{3,i} \$_{3,i} + \dot{\theta}_{4,i} \$_{4,i} + \dot{\theta}_{5,i} \$_{5,i} + \dot{\theta}_{6,i} \$_{6,i} \tag{4}$$

where ω and υ denote the angular velocity and linear velocity of the moving platform, respectively. $\dot{\theta}_{j,i}$ represents the angular velocity of the i-th branched chain j-th (j=1,2,3,4,5,6) rotational joint, and $\dot{q}_i$ denotes the active joint rates.

The unit motion screw of joint in each actuation branched chain can be obtained by

$$\begin{cases} \$_{1,i} = [\mathbf{0}; s_{i0}] \\ \$_{j,i} = [s_{j,i}; (a_i + l_i) \times s_{j,i}] \quad j = 2,3 \\ \$_{j,i} = [s_{j,i}; a_i \times s_{j,i}] \quad j = 4,5,6 \end{cases} \tag{5}$$

If the active prismatic joint of the i-th (i=1,2, 3) is locked, the additional reciprocal screw of the chain can sequentially be determined as

$$\$_i^r = \begin{bmatrix} \mathbf{l}_{i0} & a_i \times \mathbf{l}_{i0} \end{bmatrix} \tag{6}$$

where $\$_i^r$ denotes a unit screw that passing the spherical joints and parallel to vector $\mathbf{l}_{i0}$.

For the reciprocal product of (6) and (4), we can obtain

$$\$_i^r \circ \$_p = \dot{q}_i \$_i^r \circ \$_{1,i} \tag{7}$$

It can be also rewritten in the matrix format

$$\mathbf{J}_x \$_p = \mathbf{J}_t \dot{\mathbf{q}} \tag{8}$$

where

$$\mathbf{J}_t = \begin{bmatrix} \mathbf{l}_{10}{}^{\mathrm{T}} \mathbf{s}_{10} & 0 & 0 & 0 \\ 0 & \mathbf{l}_{20}{}^{\mathrm{T}} \mathbf{s}_{20} & 0 & 0 \\ 0 & 0 & \mathbf{l}_{30}{}^{\mathrm{T}} \mathbf{s}_{30} & 0 \\ 0 & 0 & 0 & \mathbf{l}_{40}{}^{\mathrm{T}} \mathbf{s}_{40} \end{bmatrix}$$

$$\mathbf{J}_x = \begin{bmatrix} \mathbf{a}_1 \times \mathbf{l}_{10} & \mathbf{a}_2 \times \mathbf{l}_{20} & \mathbf{a}_3 \times \mathbf{l}_{30} & \mathbf{a}_4 \times \mathbf{l}_{40} \\ \mathbf{l}_{10} & \mathbf{l}_{20} & \mathbf{l}_{30} & \mathbf{l}_{40} \end{bmatrix}^{\mathrm{T}}$$

Therefore, the generalized Jacobian matrix $\mathbf{J}_p$ of the parallel component can be expressed as

$$\mathbf{J}_p = \mathbf{J}_t^{-1} \cdot \mathbf{J}_x \tag{9}$$

D. Jacobian matrix of the serial component

The Jacobian matrix of the middle constrained UP branched chain can be established by D-H method [23]-[24], the joint parameters can be shown in Table I, the detailed derivation process is shown in my previous work [17].

TABLE I: D-H PARAMETERS OF THE CONSTRAINED BRANCH

i	θ_i / (°)	d_i	a_i	α_i / (°)
0	90	h	0	90
1	θ_1	0	0	90
2	θ_2	0	0	0
3	0	d_3	0	0

where θ_1 and θ_2 represent rotations angle of the universal joint, d_3 denotes the moving linear distance of the chain along the slide rail, and h denotes the distance between the two fixed platforms, yet $h = \tan\alpha(r_b - r_c)$.

From the Table I we can know, the homogeneous coordinate transformation matrix from the coordinate system *B-xyz* to the coordinate system *A-uvw* can be written as

$$\mathbf{T} = \mathbf{T}_0(h)\mathbf{T}_1(\theta_1)\mathbf{T}_2(\theta_2)\mathbf{T}_3(d_3) = \begin{bmatrix} \mathbf{R} & \mathbf{r} \\ 0 & 1 \end{bmatrix} \tag{10}$$

where

$$\mathbf{R} = \begin{bmatrix} \mathrm{s}\theta_2 & 0 & -\mathrm{c}\theta_2 \\ \mathrm{c}\theta_1\mathrm{c}\theta_2 & \mathrm{s}\theta_1 & \mathrm{c}\theta_1\mathrm{s}\theta_2 \\ \mathrm{s}\theta_1\mathrm{c}\theta_2 & -\mathrm{c}\theta_2 & \mathrm{s}\theta_1\mathrm{s}\theta_2 \end{bmatrix}, \ \mathbf{p} = \begin{bmatrix} -d_3\mathrm{c}\theta_2 \\ d_3\mathrm{c}\theta_1\mathrm{s}\theta_2 \\ d_3\mathrm{s}\theta_1\mathrm{s}\theta_2 + h \end{bmatrix}$$

Consequently, substituting (10) into (1) results in

$$\begin{cases} d_3 = \sqrt{x^2 + y^2 + (z-h)^2} \\ \theta_2 = a\mathrm{c}(-\dfrac{x}{d_3}) \\ \theta_1 = a\tan 2(\dfrac{z-h}{d_3\mathrm{s}\theta_2}, \dfrac{y}{d_3\mathrm{s}\theta_2}) \end{cases} \tag{11}$$

The mapping relationship of the UP branched chain can be formulated as

$$\mathbf{J}_{\mathbf{s}} \dot{\boldsymbol{\theta}} = \$_p \tag{12}$$

where

$$\dot{\boldsymbol{\theta}} = \begin{bmatrix} \dot{\theta}_1 & \dot{\theta}_2 & \dot{d}_3 \end{bmatrix}^{\mathrm{T}}$$

Then the Jacobian matrix of the constrained UP branched chain (serial component) can be expressed as

$$\mathbf{J}_s = \begin{bmatrix} 0 & d_3\mathrm{s}\theta_2 & -\mathrm{c}\theta_2 \\ -d_3\mathrm{s}\theta_1\mathrm{s}\theta_2 & d_3\mathrm{c}\theta_1\mathrm{c}\theta_2 & \mathrm{c}\theta_1\mathrm{s}\theta_2 \\ d_3\mathrm{c}\theta_1\mathrm{s}\theta_2 & d_3\mathrm{s}\theta_1\mathrm{s}\theta_2 & \mathrm{s}\theta_1\mathrm{s}\theta_2 \\ 1 & 0 & 0 \\ 0 & \mathrm{s}\theta_1 & 0 \\ 0 & -\mathrm{c}\theta_1 & 0 \end{bmatrix} \tag{13}$$

By employing the relationship between the parallel component Jacobian matrix and the serial component Jacobian matrix, the dimension can be normalized

$$\$_p = \mathbf{J}_q \begin{bmatrix} \dot{x} \\ \dot{y} \\ \dot{z} \end{bmatrix} \tag{14}$$

where

$$\mathbf{J}_q = \begin{bmatrix} 0 & -\frac{\mathrm{s}\theta_1}{d_3\mathrm{s}\theta_2} & \frac{\mathrm{c}\theta_1}{d_3\mathrm{s}\theta_2} \\ \frac{\mathrm{s}\theta_1\mathrm{s}\theta_2}{d_3} & \frac{\mathrm{s}\theta_1\mathrm{c}\theta_1\mathrm{c}\theta_2}{d_3} & \frac{\mathrm{c}\theta_1\mathrm{s}^2\theta_1}{d_3} \\ -\frac{\mathrm{c}\theta_1\mathrm{s}\theta_2}{d_3} & -\frac{\mathrm{c}^2\theta_1\mathrm{c}\theta_2}{d_3} & -\frac{\mathrm{s}\theta_1\mathrm{c}\theta_1\mathrm{c}\theta_2}{d_3} \\ 1 & 0 & 0 \\ 0 & 1 & 0 \\ 0 & 0 & 1 \end{bmatrix}$$

Combining the (9) and (14), the dimensionally homogeneous Jacobian matrix of the proposed parallel manipulator with a full rank, i.e. three, can be expressed as

$$\mathbf{J} = \mathbf{J}_p\mathbf{J}_q \tag{15}$$

III. The Dexterity Indices of the Parallel Manipulator

If considering the application field and working requirements of the mechanism, the condition number and manipulability of the parallel manipulator are introduced as the performance evaluation indices to estimate the dexterity.

A. Condition Number Index

The dimension of equation (15) is unified and it has been normalized for consistency in angular and linear units. So we can use the reciprocal of the condition number of the Jacobian matrix that characterizing the mapping relationship between operation velocity and the joint velocity [25]-[26], that is

$$\kappa = 1/\kappa(\mathbf{J}) \tag{16}$$

where $\kappa(\mathbf{J})$ denotes the condition of the Jacobian matrix, and $\kappa(\mathbf{J}) = \|\mathbf{J}\|\|\mathbf{J}^{-1}\|$. The value κ varies in a certain range [0, 1]. When $\kappa = 0$ shows that the configuration is in a singular position. While $\kappa = 1$ shows that the configuration is isotropic, and the mechanism has the best motion transmission property.

On the basis of the reachable workspace, this paper defines the optimum condition number region which can be reached by some configurations and satisfy the constraint condition $\kappa \geq 0.6$ [27]-[28].

B. Manipulability Index

Yoshikawa define the determinant value of the product of the Jacobian matrix and its transpose matrix as the manipulability index of the parallel manipulator [20].

$$\mu = \sqrt{\det(\mathbf{J}\cdot\mathbf{J}^T)} \tag{17}$$

The manipulability index indicates the dexterity and comprehensive performance of the parallel manipulator in all directions. When the mechanism is in a nonsingular position, the manipulability is the determinant value of the Jacobian matrix. When the mechanism approaches the singular position, the manipulability is zero, and here the Jacobian matrix belongs to the morbid matrix, whose inverse matrix precision is reduced, and the transmission performance is very poor, so that the mapping relationship between the input and output is distorted, therefore, the special configuration should be avoided in the working process.

In order to evaluate the manipulability of the parallel manipulator comprehensively and systematically, *Frobenius-norm* and *Infinity-norm* are proposed

$$\left\|\mathbf{J}\cdot\mathbf{J}^T\right\|^F = \left(\sum_{i=1}^{m}\sum_{j=1}^{n}\left|a_{i,j}\right|^2\right)^{\frac{1}{2}} \tag{18}$$

$$\left\|\mathbf{J}\cdot\mathbf{J}^T\right\|^\infty = \max_i\sum_{j=1}^{n}\left|a_{i,j}\right| \tag{19}$$

where $\left\|\mathbf{J}\cdot\mathbf{J}^T\right\|^F$ is the square of the absolute value of the matrix element and re-seeking the square root of arithmetic. While $\left\|\mathbf{J}\cdot\mathbf{J}^T\right\|^\infty$ is the maximum of the sum of absolute values of all row elements.

In general, the inverse of its norm can be formulated as the performance evaluation index, that is

$$\mu^F = \frac{1}{\left\|\mathbf{J}\cdot\mathbf{J}^T\right\|^F} \tag{20}$$

$$\mu^\infty = \frac{1}{\left\|\mathbf{J}\cdot\mathbf{J}^T\right\|^\infty} \tag{21}$$

The larger the value is, the greater the distance is away from the singular configuration, and the better dexterity of the parallel manipulator is.

IV. Cases Analysis

As a case application analysis for the parallel manipulator presented in this paper, the condition number and the manipulability are considered in this section. The structure parameters of 3-PUS-UP parallel manipulator are listed as follows: the radius of the fixed platform is r_b=750*mm*, the radius of the moving platform is r_a=250*mm*, the constant rod is *l*=700*mm*, the structure angle is $\alpha = 45^\circ$, the search range of the workspace is $-300 \leq x \leq 300$, $-300 \leq y \leq 300$, $450 \leq z \leq 1000$. The software MATLAB can be used to depict the relevant performance atlases.

A. Condition Number Analysis

Fig. 3 illustrates the distribution of the condition number under ideal workspace. From the Fig. 3, we can see that the position of the middle plane with coordinate height is *z*=850*mm*. In the range [700,850], the higher the height is, the closer the condition number of the parallel manipulator is close to 1, which indicates that the kinematic dexterity of the mechanism is much better, and the kinematic accuracy is higher. In the range [850, 1000], with the height increasing, the condition number gradually decreases, indicating the dexterity of the parallel manipulator is getting worse. However, in the search space, the range of the condition number varies between 0.35 and 0.98, indicating that the parallel manipulator has no singular configuration in the ideal workspace.

Utilizing the results of calculation, the contour distribution of the condition number κ in the reachable workspace with consideration of the limit of the actuators stroke and

rotational joint angle is evaluated and in Fig.4. As we can see that the distribution of the condition number κ ranges from 0.5 to 0.8 and is far away from the ill condition region, so the proposed parallel manipulator has good kinematic dexterity in the whole reachable workspace.

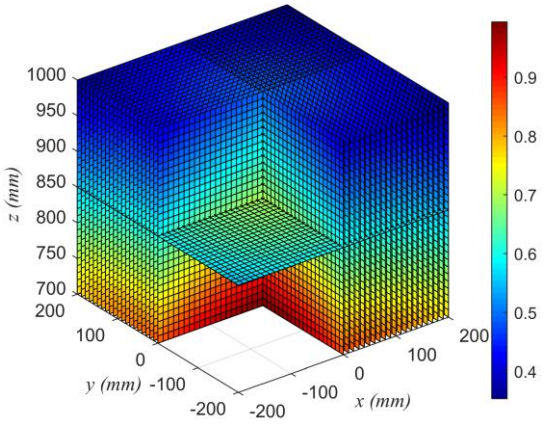

Fig. 3. The ideal workspace of condition number

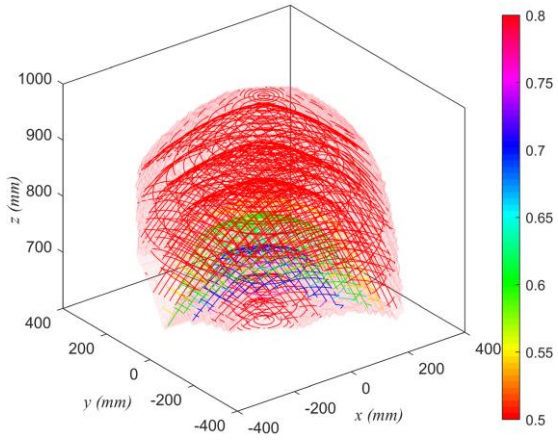

Fig. 4. The contour line of condition number in reachable workspace

Fig. 5 gives the optimum region of the condition number $\kappa \geq 0.6$ in the reachable workspace. It is vital kernel issue when we explore the trajectory planning of the parallel manipulator, we should try to determine the optimum position of a predefined path to be followed by the moving platform and execute task work in the optimum region to achieve their full potential kinematic performance.

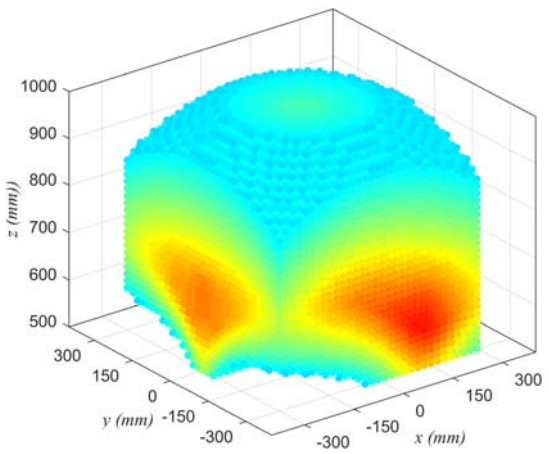

Fig. 5. The optimum region of condition number in reachable workspace

B. Manipulability Analysis

Fig.6 shows the contour line of the manipulability index μ of the 3-PUS-UP parallel manipulator under the height z=850mm, the variable range of μ is [0.6,0.69], the greater the value is, the better the dexterity of the parallel manipulator is, which indicate that the mechanism is far away from the singular configuration. The region of $\mu \geq 0.64$ is defined in this study as the optimum region and enclosed by the magenta line is a good quality region of the manipulability μ . Simultaneously, to some extent, the atlas is symmetry about the y axis.

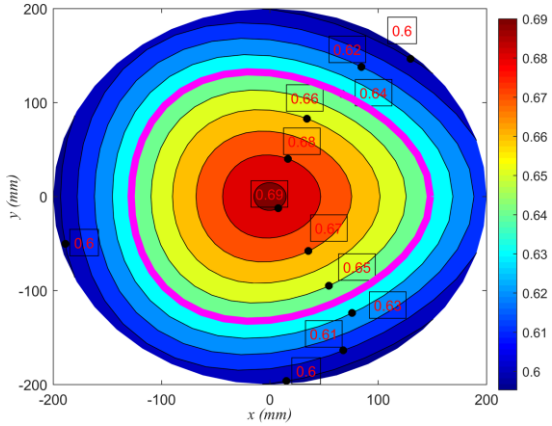

Fig. 6. The optimum region of manipulability at z=850mm.

Fig. 7 shows the contour line of the manipulability index μ^F of the 3-PUS-UP parallel manipulator under the height z=850mm, the range of μ^F is [0.8, 0.88], the greater the value is, the better the dexterity of the parallel manipulator is, which indicate that the mechanism is far away from the singular configuration. The region of $\mu^F \geq 0.83$ enclosed by the magenta line is a good quality region of the manipulability μ^F . The manipulability values indicates that the parallel manipulator has good transmission performance. Simultaneously, the atlas is symmetry about the x axis.

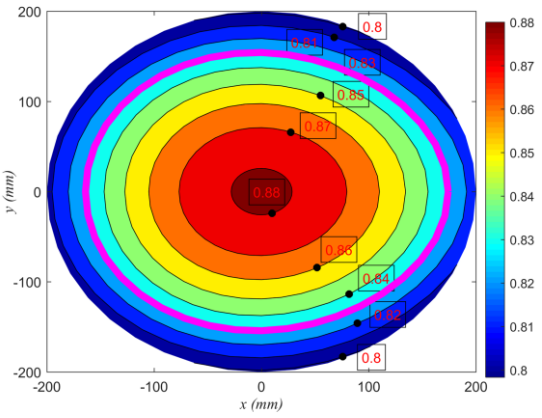

Fig. 7. The optimum region of Frobenius-norm at z=850mm

Fig. 8 shows the distribution of the manipulability index μ^∞ of the 3-PUS-UP parallel manipulator under the height z=850mm, the range of μ^∞ is [0.85, 1.1], the greater the value is, the better the dexterity of the parallel manipulator is, which indicate that the mechanism is far away from the singular configuration. The region of $\mu^\infty \geq 0.95$ enclosed by

the magenta line is a good quality region of the manipulability μ^{∞}. Simultaneously, the shape of the optimum region is triangular, which is consistent with the geometric structural characteristics of the parallel manipulator.

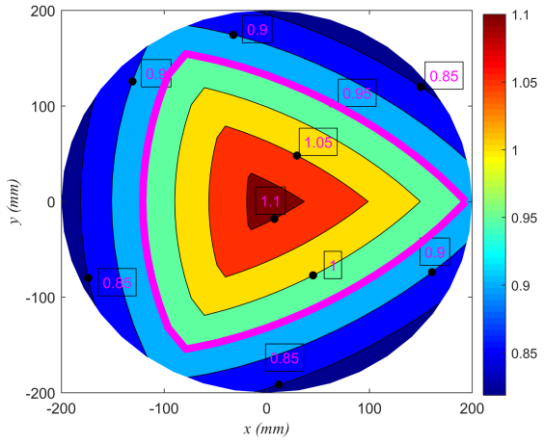

Fig. 8. The optimum region of Infinity-norm at z=850mm.

Fig. 9 illustrates the optimum region of the parallel manipulator considering the manipulability index μ, μ^{F}, and μ^{∞}. The closer to the boundaries of the workspace, the lower the manipulability performance values of the parallel manipulator. The region close to the middle of the workspace is where the more satisfactory values are calculated.

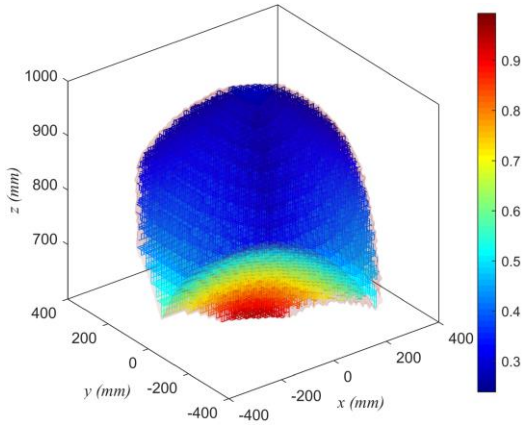

Fig. 9. The optimum region of three manipulability in reachable workspace.

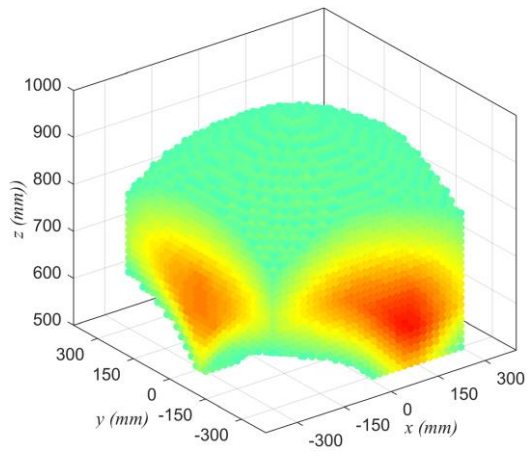

Fig. 10. The optimum region of the parallel manipulator

As illustrated in Fig.10, the optimum region and the distribution of the parallel manipulator considering all the proposed performance indices, i.e. condition number, manipulability, the Frobenius-norm, and the Infinity-norm. To design a control trajectory planning of the proposed parallel manipulator for next stage, the optimum region has to be identified so as to exert the excellent transmission performance. The results also show that the parallel manipulator has a rather good dexterity which is suitable for large components machining demands.

V. Conclusions

In this paper, a spatial three-degree of freedom 3-PUS-UP parallel manipulator with constrained branch is proposed, the parallel manipulator can be combined with the series module to perform a five degrees of freedom hybrid manipulator to execute free-surface machining. The following conclusions have been achieved in this research:

(1) A very good transformation approach to derive the dimensionally homogeneous Jacobian for dexterity analysis of the 3-PUS-UP parallel manipulator is investigated in detail.

(2) In term of the actuation and constraint relationship of the parallel manipulator, the position inverse solution is carried out, and the complete dimensionally homogeneous Jacobian matrix of the parallel manipulator is constructed systematically by virtue of the screw theory and the D-H method. The mathematical model of the performance evaluation of the parallel manipulator is deduced in detail by employing the condition number and the manipulability as the design criterion for the performance evaluation.

(3) The distribution of the dexterity in the reachable workspace based on the Jacobian matrix, as well as the optimum region of the comprehensive kinematic performance are systematically analyzed. The results illustrate that the mechanism has good kinematic dexterity and can be widely applied to precision assembly, hybrid machine, auto-mobile spraying, and so on. What's more, the present work is extremely valuable for further dynamics modeling and control design of the proposed manipulator.

Acknowledgment

The authors would like to acknowledge the financial support of the Fundamental Research Funds for the Central Universities under Grant No.2018JBZ007, No.2018YJS136, No.2017YJS158, China Scholarship Council (CSC) under Grant No.201807090079, and the National Natural Science Foundation of China (NSFC) under Grants 51675037.

References

[1] Y. G. Li, E. J. Zhang, and Y. M. Song, "Stiffness modeling and analysis of a novel 4-DOF PKM for manufacturing large components," *Chinese Journal of Aeronautics*, vol. 26, no. 4, pp. 1577-1585, 2013.

[2] F. G. Xie, X. J. Liu, and Z. You, "Type synthesis of 2T1R-type parallel kinematic mechanisms and the application in manufacturing," *Robotics and Computer Integrated Manufacturing*, vol. 30, no. 1, pp. 1-10, 2014.

[3] H. Nigatu and M. Gurala, "Dynamic and stiffness modeling of new 3DOF PKM for high speed machining application," *International Journal of Engineering and Technology Sciences*, vol.3, pp.2308-2315, 2014.

[4] X. Chen, X. J. Liu, and F. G. Xie, "A comparison study on motion/force transmissibility of two typical 3-DOF parallel manipulators: The sprint Z3 and A3 tool heads," *International Journal of Advanced Robotic Systems*, vol. 11, pp. 1-11, 2014.

[5] Y. Wang, H. Liu, and T. Huang, “Stiffness modeling of the tricept robot using the overall Jacobian matrix,” *Journal of Mechanism and Robotics*, vol. 1, no. 2, pp. 1-8, 2009.
[6] J. Zhang, Y. Zhao, and Y. Jin, “Elastic-dynamic modeling and analysis for an Exechon parallel kinematic machine,” *Journal of Manufacturing Science and Engineering,* vol. 138, no. 3, pp. 1-14, 2016.
[7] C. L. Chen, H. T. Liu, and T. Huang, “Kinematic performance analysis of redundantly 4-UPS&UP parallel manipulator,” *Journal of Mechanical Engineering*, vol. 52, no. 5, pp. 124-129, 2016.
[8] Y. Lu, B.Hu, “Analyzing kinematics and solving active/constrained forces of a 3SPU+UPR parallel manipulator,” *Mechanism and Machine Theory*, vol. 42, no. 10, pp. 1298-1313, 2007.
[9] S. M. Kim, B. J. Yi, and J. Cheong, “Implementation of a revolute-joint-based asymmetric Schönflies motion haptic device with redundant actuation,” *Mechatronics*, vol. 50, pp. 87-103, 2018.
[10] Y. Hu, B. Li, “Robust design and analysis of 4PUS-1RPU parallel mechanism for a 5-degree-of-freedom hybrid kinematics machine,” in *Proc. the Institution of Mechanical Engineers Part B Journal of Engineering Manufacture*, vol. 225, no. 5, pp. 685-698, 2011.
[11] H. Nigatu and M. Gurala, “Dynamic and stiffness modeling of new 3DOF PKM for high speed machining application,” *International Journal of Engineering and Technology Sciences*, vol. 3, pp. 2308-2315, 2014.
[12] H. Q. Zhang and H. R. Fang, "Stiffness characteristics analysis of a novel 3- DOF parallel kinematic machine tool," *International Journal of Engineering and Technology*, vol. 10, no. 4, pp. 346-354, 2018.
[13] Y. Wang, T. Huang, D. G. Chetwynd, “Analytical method for stiffness modeling of the tricept robot,” *Journal of Mechanical Engineering*, vol. 44, no. 38, pp. 13-19, 2008.
[14] T. Huang, M. Li, and M. Wu, “Criteria for conceptual design of reconfigurable PKM modules theory and application,” *Journal of Mechanical Engineering*, vol.41, no.8, pp. 36-41, 2005.
[15] Q. C. Li, X. X. Chai, and Q. H. Chen, “Review on 2R1T 3-DOF parallel mechanisms,” *Chinese Science Bulletin*, vol. 41, pp. 1507-1519, 2017.(in Chinese)
[16] Z. Gao and D. Zhang, “Performance analysis, mapping, and multiobjective optimization of a hybrid robotic machine tool,” *Industrial Electronics IEEE Transactions on*, vol. 62, no. 1, pp. 423-433 2015.
[17] G. H. Cui, H. Q. Zhang, and F. Xu, “Kinematic dexterity and stiffness performance of spatial 3-PUS-UP parallel manipulator,” *Transactions of Chinese Society for Agricultural Machinery*, vol. 45, no.12, pp. 348-354, 2014.
[18] J. P. Merlet, “Jacobian, manipulability, condition number and accuracy of parallel robots,” *Robotics Research*. Springer Berlin Heidelberg, pp.199-206, 2007.
[19] T. Huang and J. S. Wang, “Closed form solution to the local dexterity and isotropy of stewart parallel manipulators,” *Chinese Journal of Mechanical Engineering*, vol.35, no.56, pp. 41-46, 1999.
[20] T. Yoshikawa, “Manipulability and Redundancy Control of Robotic Mechanisms,” in *Proc. IEEE International Conference on Robotics and Automation*, 2003, pp. 1004-1009.
[21] Y. Lu, B. Hu, and P. L. Liu, “Kinematics and dynamics analyses of a parallel manipulator with three active legs and one passive leg by a virtual serial mechanism,” *Multibody System Dynamics*, vol. 17, no. 4, pp. 229-241, 2007.
[22] A. Wu, Z. Shi, and X. Yang, “Formalization and analysis of jacobian matrix in screw theory and its application in kinematic singularity,” in *Proc. International Conference on Intelligent Robots and Systems*. IEEE, 2017, pp. 2835-2842
[23] J. Guo and J. Ni, “Kinematics and statics analysis of dexterous hand,” in *Proc. International Conference on Mechatronics, Control and Materials*, vol.104, pp. 260-265, 2016.
[24] S. Joshi and L. W. Tsai, “A comparison study of two 3-DOF parallel manipulators: One with three and the other with four supporting legs,” *IEEE Transactions on Robotics and Automation*, vol. 19, no. 2, pp. 2 00-209, 2003.
[25] C. Gosselin and J. Angeles, “A global performance index for the kinematic optimization of robotic manipulator,” *Journal of Mechanical Design*, vol. 113, no. 3, pp. 220-226, 1991.
[26] P. Geoffrey and J. A. Carretero, “Formulating jacobian matrices for the dexterity analysis of parallel manipulators,” *Mechanism and Machine Theory*, vol. 41, no. 12, pp. 1505-1519, 2006.
[27] G. Cui, D. Zhang, and H. Zhou, “Operating dexterity optimization and analysis of a 3-DOF parallel manipulator for a tunnel segment assembly system,” *International Journal of Mechanics and Materials in Design*, vol.11, no. 3, pp. 277-285, 2015.
[28] J. Wu, J. Wang, and Z. You, “A comparison study on the dynamics of planar 3-DOF 4-RRR, 3-RRR and 2-RRR parallel manipulators,” *Robotics and Computer Integrated Manufacturing*, vol. 27, no. 1, pp. 150-156, 2011.

Haiqiang Zhang is a PhD student in the school of Beijing Jiaotong University, Beijing, China from 2015. In 2018, he receives the China Scholarship Council (CSC) Founding to York University as a joint PhD student. He received the master degree in mechanical engineering from Hebei University of Engineering in 2015 and the bachelor degree in mechanical design and theories from Yantai University in 2012. His primary research interest is focus on robotics in computer integrated manufacturing, parallel kinematics machine tool, redundant actuation robots, over-constrained parallel manipulators, and multi-objective optimization design, and so on.

Hairong Fang received the bachelor degree in mechanical engineering from Nanjing University of Science and Technology in 1990, master degree in mechanical engineering from Sichuan University in 1996, and a PhD degree in mechanical engineering from Beijing Jiaotong University in 2005, respectively. She worked as Associate Professor in the Department of Engineering Mechanics at Beijing Jiaotong University, Beijing, China, from 2003 to 2011. She is a professor in the School of Mechanical Engineering from 2011 and director of robotics research center. Her primary research interests in parallel mechanisms, digital control, robotics and automation, machine tool equipment, and green manufacturing.

Bingshan Jiang received a bachelor degree in mechanical electronic engineering from Liaoning Technical University, Fuxin, China in 2015, and the master degree in mechanical engineering from Liaoning Technical University, Fuxin, China in 2017. He is currently a candidate of PhD at School of Mechanical, Electronic and Control Engineering, Beijing Jiaotong University, Beijing, China.

His research interests include synthesis, kinematics, dynamics and control of parallel robots.

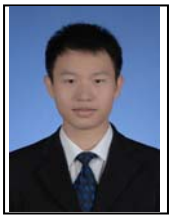

Shuaiguo Wang received the bachelor degree in mechanical engineering and automation from Changchun University of Technology in 2015.

His research interests include principle and method of automatic control, automation unit technology and integration technology and its application in all kinds of control systems, robot system integration, and automobile automation production line.